


Distributed and reliable decision-making for cloud-enabled mobile service platforms

International Journal of Distributed
Sensor Networks
2017, Vol. 13(8)
© The Author(s) 2017
DOI: 10.1177/1550147717726509
journals.sagepub.com/home/ijdsn


Joongheon Kim¹ and Aziz Mohaisen²

Abstract

This article proposes distributed decision-making algorithms for reliable operation in cloud-assisted social network architectures. The considered architecture consists of three types of units: a cloud platform, access units, and mobile units (MUs). For reliable operations in such architectures, two distributed decision-making algorithms are proposed: (1) *decision-making for fair connection at MUs* and (2) *decision-making for dynamic buffering at access units*. For the decision-making in fair connection at MUs, the deployed MUs find their new access units to be associated with them when currently associated access units are out of order. The proposed algorithm works considering buffer backlog in access units, achievable rates with access units, and the number of associated MUs in access units. For the decision-making in dynamic buffering at access units, the buffers in access units are dynamically controlled for time-average expected power consumption minimization (i.e. energy-efficiency maximization) subjected to buffer stability.

Keywords

Fair connection, buffer control, social networks, cloud computing, decision-making

Date received: 24 December 2016; accepted: 13 July 2017

Academic Editor: Myungsik Yoo

Introduction

Social networks have emerged recently to be one of the most popular distributed computing paradigms,¹ making the social network service (SNS) platform as one of the most essential networking architectures.^{2–5} Since the SNS data are stored in cloud-based centralized storage, the corresponding wireless text, image, and video data flow management from SNS mobile units (MUs) to a cloud platform (CP) storage is of great interest. In addition, to deliver data from the SNS MUs to a CP, intermediate access units (AUs) are required. Since millimeter-wave (mmWave) wireless backhaul and access communications have been widely studied,⁶ the connections between (1) AUs and a CP and (2) AUs and MUs should be established over mmWave wireless channels.

In this given network architecture, which includes a CP, AUs, and MUs, each AU is associated with

multiple MUs with various scheduling policies. In addition, backhaul links between AUs and a CP generally utilize a 60-GHz channel.⁶ Furthermore, access links between AUs and MUs generally use 28 or 38 GHz channels which have been studied for the 5G cellular network architectures.^{7–9} For reliable operations in this cloud-assisted SNS platform, two distributed decision-making algorithms are proposed in this article: (1) *decision-making for fair connection in each MU* and (2)

¹School of Computer Science and Engineering, Chung-Ang University, Seoul, Republic of Korea

²Department of Computer Science, University of Central Florida, Orlando, FL, USA

Corresponding author:

Aziz Mohaisen, Department of Computer Science, University of Central Florida, 4328 Scorpis Street, Building 116 Room 346, Orlando, FL 32816, USA.

Email: mohaisen@iee.org



decision-making for dynamic buffering in each AU. In this article, the definition of *reliability* is used as an equivalent to *buffer stability*, mainly because a system would become unstable if it starts to lose information by queue overflow. In fair connection, we consider the fairness among the buffers in order to avoid overflow. In addition to this contribution, a novel dynamic buffering algorithm is introduced in this article, this avoiding buffer overflow.

For designing a *fair connection decision-making algorithm in each MU*, this article considers the cases where (1) some AUs have unexpectedly failed (i.e. out of service; equivalent to churn out) or (2) new MUs join the network at some point during the operation of the network. With traditional connection (or association) algorithms, each MU finds its own new access point (AP) which is able to provide the highest received signal strength (RSS).¹⁰ However, considering only RSS is not enough for fair connection. In particular, the proposed fair algorithm considers additional factors, such as (1) the buffer backlog in each AU to avoid overflows, (2) the number of associated MUs in each AU to consider scheduling impacts, and (3) bandwidth in 28 and 38 GHz channels.

For designing a *dynamic buffering decision-making algorithm in each AU*, this article determines transmit power allocation in each AU to send data from each AU to its associated CP. Note that the transmit power allocation is associated with buffer backlog in each AU. If the transmit power in each AU is static and too small, the number of transmitted bits from the AU becomes small, that is, the AU has higher buffer-overflow probability. However, if the transmit power in each AU is static and possibly too big, the buffer can be stable, although it is energy-inefficient. Therefore, a dynamic buffering algorithm is designed based on the buffer backlog in each AU over 60 GHz links.

Organization

The rest of this article is organized as follows. Section “Preliminaries” reviews the preliminaries of this work. Section “Reliable decision-making” presents the proposed distributed algorithms for reliable cloud-assisted SNS platforms. Section “Performance evaluation” evaluates the performance of the proposed algorithms. Section “Concluding remarks and future work” draws concluding remarks.

Preliminaries

This section reviews the preliminaries of this work, including a reference network model (section “Reference SNS CPs”), wireless propagation characteristics (section “Propagation characteristics”), motivation of this work

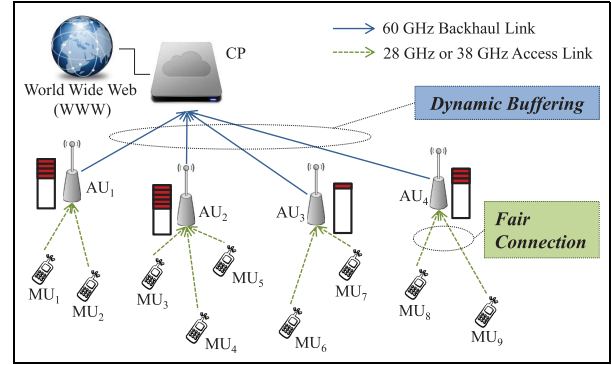


Figure 1. A reference social network cloud platform: each MU (a social network user) uploads its own data to a CP and the CP shares the data to the MU’s neighbors via World Wide Web.

(section “Motivation”), and a review of the related work (section “Related work”).

Reference SNS CPs

As shown in Figure 1, the SNS CP considered in this study consists of a CP, AUs, and MUs, where the CP is connected to all deployed AUs via 60 GHz backhaul links.⁶ Each MU uploads its data to a CP via its associated AU for SNS data sharing. When the data are uploaded, the CP stores the data and shares them with the MU’s SNS neighbors or friends via World Wide Web (WWW). Therefore, the CP works as centralized controller which manages packet flows in the entire networks.^{11–13} In addition, each MU is associated with only one AU under the assumption that each MU has one antenna due to its hardware limitations. Each AU can be associated with multiple MUs with scheduling policies. Each AU_{*i*} also broadcasts the information of the number of associated MUs, $N_i[t]$, at each time. Each AU uses 28 or 38 GHz radios to talk with its associated MUs.^{7,8,14} The main characteristic of this SNS CPs is to do with high sensitivity and demand for real-time properties. Different from existing techniques in the domain is that our technique could be very suitable where not only real-time consumption of multimedia would be useful but also uploading is done in real time. Therefore, the proposed algorithms in this article for reliable operations are especially meaningful because of their control of buffers for reliability in real time, which suites such systems.

Suppose that there exist the number of AUs in reference cloud-assisted SNS platforms, \mathcal{N}_{AU} . For each AU_{*i*} where $\forall i \in \{1, \dots, \mathcal{N}_{AU}\}$, buffer dynamics in each time $t \in \{0, 1, \dots\}$ are characterized as follows (also illustrated in Figure 2)

$$B_i[t + 1] = (B_i[t] - \mu_i[t] + \lambda_i[t])^+ \quad (1)$$

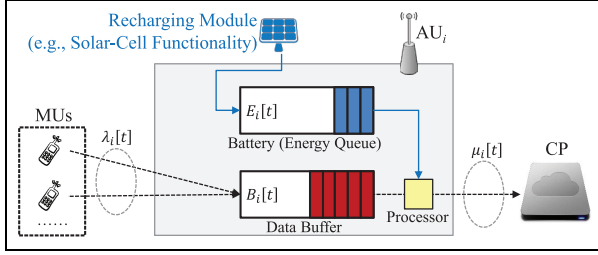


Figure 2. Illustration of the buffer dynamics in an AU_i where $\lambda_i[t]$ and $\mu_i[t]$ are the arrival and departure processes of the buffer $B_i[t]$, respectively. The $E_i[t]$ in AU_i stands for the energy level at time t . The processor of AU_i can process bits from $B_i[t]$ as much as the $E_i[t]$ allows due to the fact that the processor capability depends on the power (or energy) allocation from $E_i[t]$.

where $(\alpha)^+ \triangleq \max\{\alpha, 0\}$; $B_i[t]$ stands for the buffer backlog in an AU_i , $\forall i \in \{1, \dots, \mathcal{N}_{AU}\}$ at t (unit: bit); $\lambda_i[t]$ stands for the number of bits arrived to an AU_i , $\forall i \in \{1, \dots, \mathcal{N}_{AU}\}$ from its associated MUs at t ; and $\mu_i[t]$ stands for the number of transmitted bits from the AU_i , $\forall i \in \{1, \dots, \mathcal{N}_{AU}\}$ to a CP at t that depends on the transmit power allocation as follows

$$\mu_i[t] = \mathcal{W}_i[t] \log_2 \left(1 + \frac{P_i^{Rx}[t]}{N_0} \right) \quad (2)$$

where $\mathcal{W}_i[t]$ is a bandwidth between AU_i , $\forall i \in \{1, \dots, \mathcal{N}_{AU}\}$ and a CP at t at 60 GHz; $P_i^{Rx}[t]$ is a received power at a CP from its associated AU_i at t ; and N_0 is a background noise.

Each AU_i , where $\forall i \in \{1, \dots, \mathcal{N}_{AU}\}$, has its own battery which is formulated as follows

$$E_i[t+1] = \left\{ (E_i[t] - \mu_i^e[t] + \lambda_i^e[t])^+ \right\}^* \quad (3)$$

where $\{\beta\}^* \triangleq \min\{E_i^{\max}, \beta\}$, $E_i[t]$ is the amount of energy (or power) within the AU_i 's battery, E_i^{\max} is the maximum energy level within the AU_i 's battery, $\mu_i^e[t]$ is the consumed energy as a result of the transmission of bits from AU_i 's buffer (i.e. $\mu_i^e[t] = P_i^{Tx}[t]$, where $P_i^{Tx}[t]$ stands for the transmit power allocation at AU_i at time t), and $\lambda_i^e[t]$ is the recharged energy using AU-equipped recharging modules. Assume that the amount of recharged energy is constant in each unit time t , and that the battery is fully charged at $t=0$, that is, $E_i[0] = E_i^{\max}$, $\forall i \in \{1, \dots, \mathcal{N}_{AU}\}$.

Propagation characteristics

Nowadays, mmWave channels are actively considered for next-generation high-capacity wireless links including 28, 38, and 60 GHz. In this article, 60 GHz channels are used for backhaul links, whereas 28 or 38 GHz channels are used for access links. For backhaul links, 60 GHz channels are used because they have the widest

wireless channel bandwidth, that is, 2.16 GHz.¹⁴ For access links, 38 or 28 GHz channels are used because they have been studied and show that they are suitable for the next-generation cellular systems.¹⁴

- (1) 60 GHz backhaul links

The 60-GHz path-loss $PL(d)$ is defined as follows¹⁵

$$A + 20 \log_{10}(f) + 10n \log_{10}(d) + \mathcal{X}_\sigma \quad (4)$$

where d is the distance between transmitter and receiver (unit: m), f is the carrier frequency in a GHz scale, A is the antenna-specific parameter depending on the beamwidth (32.5 dB in line-of-sight (LoS) and 51.5 dB in non-LoS (NLoS)), n is the path-loss coefficient (2.0 in LoS and 0.6 in NLoS), and \mathcal{X}_σ is a shadowing effect in NLoS and it is represented as a Gaussian distribution with 0 mean and 3.3 dB standard deviation, respectively. Obviously, $\mathcal{X}_\sigma = 0$ in LoS.

Based on equation (4), the received signal power at a CP from AU_i can be calculated as follows

$$P_i^{Rx}[t] = 10 \left(\frac{G_i^{Tx} + G_j^{Rx} - \alpha(d) - PL(d) + 10 \log_{10} P_i^{Tx}[t]}{10} \right) \quad (5)$$

$$= \mathcal{D}(G_i^{Tx}, G_j^{Rx}, d) P_i^{Tx}[t] \quad (6)$$

where $\mathcal{D}(G_i^{Tx}, G_j^{Rx}, d)$ is defined as follows

$$\mathcal{D}(G_i^{Tx}, G_j^{Rx}, d) \triangleq \frac{10^{\frac{G_i^{Tx} + G_j^{Rx}}{10}}}{10^{\frac{\alpha(d) + PL(d)}{10}}} \quad (7)$$

where $P_i^{Tx}[t]$ in equation (6) is the transmit power at an AU_i , $\forall i \in \{1, \dots, \mathcal{N}_{AU}\}$, to a CP; G_i^{Tx} is the transmit antenna gain at an AU_i , $\forall i \in \{1, \dots, \mathcal{N}_{AU}\}$; G_j^{Rx} is the receive antenna gain at a CP; and $O(d)$ is the oxygen attenuation (16 dB/Km¹⁶).

- (1) 38 or 28 GHz access links

The 38- and 28-GHz path-loss models $PL(d)$ are as follows^{7,8}

$$20 \log_{10} \left(\frac{4\pi d_0}{\lambda} \right) + 10n \log_{10} \left(\frac{d}{d_0} \right) + \mathcal{X}_\sigma \quad (8)$$

where d , d_0 , λ , n , and \mathcal{X}_σ stand for the distance between a transmitter and a receiver, reference distance (5.0 m in Rappaport et al.⁷), wavelengths (7.78 mm in 38 GHz⁷ and 10.71 mm in 28 GHz⁸), average path-loss coefficient over distance, and shadowing random variable which is represented as a Gaussian random variable with 0 mean and σ standard deviation. n and σ values in 38 and 28 GHz are measured in Rappaport et al.⁷ and Azar et al.,⁸ and summarized in Table 1.

Table 1. Path-loss exponents (n) and standard deviations of shadowing (σ).^{7,8}

Configuration	n	σ
25 dBi antenna at 38 GHz (LoS)	2.20	10.3
25 dBi antenna at 38 GHz (NLoS)	3.88	14.6
13.3 dBi antenna at 38 GHz (LoS)	2.21	9.40
13.3 dBi antenna at 38 GHz (NLoS)	3.18	11.0
24.5 dBi antenna at 28 GHz (LoS)	2.55	8.66
24.5 dBi antenna at 28 GHz (NLoS)	5.76	9.02

Note that the oxygen attenuation is negligible in 38 or 28 GHz radios (<0.1 dB/Km).¹⁶

Motivation

In the reference cloud-assisted SNS platform, there are two potential issues that may affect the robust network operations: (1) the potential of AU breaking down and (2) buffer management in each AU, which affects its stability. In the following, both issues are discussed, which are the motivation of this work.

If an AU breaks down, its associated MUs should find new AUs. In traditional association algorithms, MUs select their own AUs which can provide the highest RSS to increase channel capacity.¹⁰ However, this can introduce a scenario where all MUs will be associated with only one AU with the highest transmit power (resulting in *association problem*). This, in turn, will cause the buffer within the AU to increase dramatically and become unstable. Therefore, it is needed to design a new association algorithm with fair connection to resolve this association problem. In such design, if the buffer backlog in an AP is almost full, it should avoid additional MU association to avoid buffer overflow. In addition, it is essential to consider different channel bandwidth parameters, since system considered in this work uses two different carrier frequencies: 28 and 38 GHz. Last but not least, if one AU serves many MUs, then the wireless spectrum should be shared by the MUs. Thus, the number of MUs should be taken into account as a design criterion. Based on all of these factors, it is required to design a fair connection algorithm in each MU (c.f. section “Decision-making for fair connection”).

As illustrated in Figure 1, each AU has its own buffer. If there are a lot of bits arriving into the buffer, more transmit power is needed to process them for stabilization. Otherwise, it requires less transmit power for energy-efficiency. Thus, stochastic buffer control is needed in each AU which aims at energy-efficiency subjected to buffer stabilization (c.f. section “Decision-making for dynamic buffering”).

Related work

The dynamic buffering algorithms have been studied in the literature, as presented in Kim and colleagues.^{15,17,18}

This section reviews such work focusing on the differences between it and this work.

The proposed algorithm in Hong and Kim¹⁷ is for joint coding and uplink transmission in cloud radio access networks (CRANs). The CRAN¹⁷ is different from the network model in this article in the sense that all MUs are connected to all AUs, and the CP does the joint processing for decoding signals from MUs.¹⁷ Therefore, CRAN does not have connection selection issues (thus, no association problem as in this work). Moreover, the algorithm in Hong and Kim¹⁷ is for the tradeoff between coding rates and delays, whereas this article is concerned with the tradeoff between energy-efficiency and delays. The proposed algorithm in Kim and Lee¹⁸ is for the uplink transmission in medical platforms. However, the proposed algorithm in Kim and Lee¹⁸ uses max-weight scheduling which makes scheduling decisions in each unit time. Such approach is a burden in WiFi networks due to handoff delays. In addition, association mechanisms are not defined in Kim and Lee.¹⁸ Moreover, the recharging mechanism is not considered either. Finally, the connection between APs and centralized storage in Kim and Lee¹⁸ is wireline (Ethernet), whereas the link is wireless in this article. The proposed algorithm in Kim¹⁵ is for downlink transmission, whereas this article considers the uplink transmission. Similar to the algorithm in Kim and Lee,¹⁸ the algorithm proposed in Kim¹⁵ does not consider recharging functionality which is essential in mobile devices. Finally, the connection between APs and centralized storage in Kim¹⁵ is wireline (Ethernet), whereas the link is wireless in this article. Thus, the considering network architecture is totally different.

Reliable decision-making

To this end, this article proposes two distributed decision-making algorithms for reliable SNS CPs: (1) *fair connection at MUs* (section “Decision-making for fair connection”) and (2) *dynamic buffering at AUs* (section “Decision-making for dynamic buffering”).

Decision-making for fair connection

As shown in Figure 3(a), deployed AUs might be broken down and thus its corresponding fault-tolerable operation is required in each MU. Therefore, the associated MUs with the broken AU should be re-associated as shown in Figure 3(b). In addition, fair connection is required when new MUs join into the network. In general, each MU_{*j*} can find its new AU which provides the maximum received signal to the MU_{*j*}.¹⁰ However, this approach is not suitable for heterogeneous 28 and 38 GHz networks because the highest RSS cannot guarantee maximum achievable rates due to bandwidth differences. Due to Shannon’s

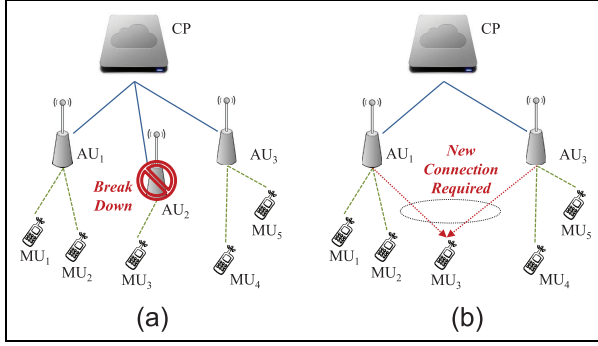


Figure 3. Illustration for fault-tolerant fair connection: (a) before and (b) after.

equation, the achievable rates from MU_j to AU_i are given as

$$C_{i \rightarrow j}[t] = W_{i \rightarrow j} \log_2 \left(1 + \frac{P_{i \rightarrow (j)}^{\text{Rx}}[t]}{N_0} \right) \quad (9)$$

where $W_{i \rightarrow j}$ is the bandwidth between AU_i and MU_j which is 800 MHz and 1.4 GHz in 28 and 38 GHz.¹⁴ In addition, $P_{i \rightarrow (j)}^{\text{Rx}}[t]$ is an RSS at MU_j from AU_i . Therefore, as observed in equation (9), even if the RSS is small in a 38-GHz channel, the channel can provide more data rates due to wider bandwidth. Furthermore, the buffer backlog $B_i[t]$ in each AU_i should be taken into account. If the $B_i[t]$ is long, it introduces delays in transmission from MUs to a CP via the AU_i . Thus, an AU which has shorter buffer backlog should be chosen with higher probability. Finally, the associated MUs in an AU share medium, that is, the rate by equation (9) should be fairly shared by all associated MUs. Therefore, the number of associated MUs in each AU_i (i.e. $N_i[t]$) should also be taken into account. Finally, the MU_j needs to find its new AU by finding the maximum $K_i[t]$, where i is an index for AUs. This $K_i[t]$ can be calculated as follows

$$\frac{W_{i \rightarrow j}}{B_i[t] \cdot (N_i[t] + 1)} \log_2 \left(1 + \frac{P_{i \rightarrow (j)}^{\text{Rx}}[t]}{N_0} \right) \quad (10)$$

The pseudo-code of this algorithmic procedure is presented in Algorithm 1. Based on Algorithm 1, the computational complexity can be calculated. As can be seen in the pseudo-code, equation (10) is computed if the conditions of churning in and out (i.e. AU breaking down and new MU joining) are satisfied. Therefore, it is a sequential calculation of one closed-form equation, that is, the complexity can be presented as $O(1)$. Finally, it is obvious that our proposed algorithm guarantees polynomial-time operations.

Fair connection at MU_j

Decision-making for dynamic buffering

This section discusses the stable data transmission from AUs to a CP. If each AU transmits data with a static rate, it may introduce overflow when the rate is too small. Otherwise, if the rate is too high, the buffer may be stable but it consumes transmit power inefficiently. Therefore, dynamic buffering is required for energy-efficient and stable buffer management.

The model in equation (2) can be simplified as follows—because only 60 GHz radio is used for backhaul

$$\mu_i[t] = W \log_2 \left(1 + \frac{P_i^{\text{Rx}}[t]}{N_0} \right) \quad (11)$$

In equation (1), $\lambda_i[t]$ is the number of bits arrived at AU_i from its associated MUs at t , that is

$$\lambda_i[t] \triangleq \sum_{k \in \mathcal{S}_{\text{MU}}^i} \mu_k^{\text{MU}}[t], \forall i \in \mathcal{S}_{\text{AU}} \quad (12)$$

where $\mathcal{S}_{\text{MU}}^i$ is the set of MUs associated with AU_i and $\mu_k^{\text{MU}}[t]$ is the transmitted bits from MU_k to its associated AU.

This section states the minimization of sum of the time-average expected power consumption of AUs as

$$\min : \sum_{i \in \mathcal{S}_{\text{AU}}} \left(\lim_{t \rightarrow \infty} \frac{1}{t} \sum_{\tau=0}^{t-1} P_i^{\text{Tx}}[\tau] \right) \quad (13)$$

and the corresponding two constraints are as follows: (1) $B_i[t], \forall i \in \mathcal{S}_{\text{AU}}$ are rate stable, that is

$$\lim_{t \rightarrow \infty} B_i[t]/t = 0, \forall i \in \mathcal{S}_{\text{AU}} \quad (14)$$

and (2) the transmit power in AU_i at t , that is, $P_i^{\text{Tx}}[t]$, has lower and upper bounds defined as

$$P_i^{\min} \leq P_i^{\text{Tx}}[t] \leq E_i[t], \forall i \in \mathcal{S}_{\text{AU}} \quad (15)$$

because $P_i^{\max}[t] = E_i[t], \forall i \in \mathcal{S}_{\text{AU}}$.

Let $\Theta(t)$ denote the column vector of all buffers in AUs at t , and define the quadratic Lyapunov function $L[t]$ as follows

$$L[t] = \frac{1}{2} \Theta^T[t] \Theta[t] = \frac{1}{2} \sum_{i \in \mathcal{S}_{\text{AU}}} B_i[t]^2 \quad (16)$$

where $\Theta^T[t]$ denotes the transpose of $\Theta[t]$. Then, let $\Delta[t]$ be defined as a conditional quadratic Lyapunov function that can be formulated as $\mathbb{E}[L[t+1] - L[t] | \Theta[t]]$, that is, the drift on t . This dynamic policy is designed to solve the given optimization formulation by observing the current buffer-backlog sizes $B_i[t]$ and determining the amount of power allocation to maximize a bound on $\mathbb{E}[P_i^{\text{Tx}}[t] | \Theta[t]] - V \Delta[t]$, where $P_i^{\text{Tx}}[t]$ is the column vector of $P_i^{\text{Tx}}[t], i \in \mathcal{S}_{\text{AU}}$, and V is a positive constant

control parameter of the policy that affects the power-delay tradeoffs.

Power control for dynamic buffering at AU_i

The proposed algorithm minimizes a bound on the $\mathbb{E}[P_i^{\text{Tx}}[t]|\Theta[t]] - V\Delta[t]$ and this in turn minimizes

$$\sum_{i \in \mathcal{S}_{\text{AU}}} \mathbb{E}[P_i^{\text{Tx}}] + V \sum_{i \in \mathcal{S}_{\text{AU}}} B_i[t](\lambda_i[t] - \mu_i[t]) \quad (17)$$

where V is a constant tradeoff factor. Then, by equations (11) and (12), equation (17) is written as follows

$$\begin{aligned} & \sum_{i \in \mathcal{S}_{\text{AU}}} P_i^{\text{Tx}}[t] + V \sum_{i \in \mathcal{S}_{\text{AU}}} B_i[t] \sum_{k \in \mathcal{S}_{\text{MU}}} \mu_k^{\text{MU}}[t] \\ & - V \sum_{i \in \mathcal{S}_{\text{AU}}} B_i[t] \mathcal{W} \log_2 \left(1 + \frac{P_i^{\text{Rx}}[t]}{N_0} \right) \end{aligned} \quad (18)$$

As shown in equation (18), it is obvious that the equation is separable, that is, if each AU minimizes its own objective function, that is

$$\begin{aligned} & P_i^{\text{Tx}}[t] + VB_i[t] \sum_{k \in \mathcal{S}_{\text{MU}}} \mu_k^{\text{MU}}[t] \\ & - VB_i[t] \mathcal{W} \log_2 \left(1 + \frac{P_i^{\text{Rx}}[t]}{N_0} \right) \end{aligned} \quad (19)$$

By equation (6), this can be further represented as follows

$$\begin{aligned} & \mathcal{F}(P_i^{\text{Tx}}[t]) \triangleq P_i^{\text{Tx}}[t] + VB_i[t] \sum_{k \in \mathcal{S}_{\text{MU}}} \mu_k^{\text{MU}}[t] \\ & - VB_i[t] \mathcal{W} \log_2 \left(1 + \frac{\mathcal{D}(G_i^{\text{Tx}}, G_C^{\text{Rx}}, d)}{N_0} P_i^{\text{Tx}}[t] \right) \end{aligned} \quad (20)$$

where G_C^{Rx} stands for the receive antenna gain at a CP. The $\mathcal{F}(P_i^{\text{Tx}}[t])$ is differentiated by $P_i^{\text{Tx}}[t]$ and it can be set to 0 to find its optimum solution, thus

$$\frac{\partial}{\partial P_i^{\text{Tx}}[t]} \mathcal{F}(P_i^{\text{Tx}}[t]) = 0 \quad (21)$$

and thus the optimum solution of $P_i^{\text{Tx}}[t]$ is obtained as

$$P_i^{\text{Tx}}[t] = \frac{\mathcal{W}V}{\ln 2} B_i[t] - N_0 \frac{10^{\frac{O(d) + PL(d)}{10}}}{10^{\frac{G_i^{\text{Tx}} + G_C^{\text{Rx}}}{10}}} \quad (22)$$

After obtaining the solution $P_i^{\text{Tx}}[t]$ by equation (22), this value should be adjusted as follows by equation (15)

$$P_i^{\text{Tx}}[t] = \min[\max\{P_i^{\text{min}}, P_i^{\text{Tx}}[t]\}, P_i^{\text{max}}[t]] \quad (23)$$

where $P_i^{\text{max}}[t] = E_i[t], \forall i \in \mathcal{S}_{\text{AU}}$.

By conducting this dynamic buffering, time-average expected power consumption minimization (alternatively,

energy-efficiency maximization) subjected to buffer stability can be guaranteed based on the theory of Lyapunov optimization and control.¹⁵

Finally, the pseudo-code of this algorithmic procedure is presented in Algorithm 2. Based on Algorithm 2, the computational complexity can be calculated as follows. As can be seen in the pseudo-code, the closed-form in equation (22) is computed in each unit time. Therefore, it is a sequential calculation of one closed-form equation, that is, the complexity can be presented as $O(1)$, meaning that the complexity of our proposed algorithm is polynomial.

Performance evaluation

This section evaluates the performance of the proposed algorithms. For this evaluation, the performance results are presented in terms of fair connection and dynamic buffering.

The performance evaluation in this article is simulation-based. In this simulation, following settings are used. Suppose that the size of the simulation network is 1000 m \times 1000 m and the network contains 1 CP and 10 AUs (5 AUs are operating at 38 GHz and the other 5 AUs are operating at 28 GHz). All AUs are randomly (and uniformly) deployed in the network. Then, the MUs randomly appear or disappear as the time goes by. In this simulation, it is assumed that all given MUs have both 28 and 38 GHz radios.

In order to run the simulation, the background noise N_0 should be precisely pre-calculated. For background noise pre-calculation, the following model is used⁹

$$N_{mW} = 10^{(k_B T_e + 10 \log_{10}(\mathcal{W}) + L_{\text{implementation}} + F_N)/10} \quad (24)$$

where $k_B T_e$ is the noise power spectral density (-174 dBm/Hz⁹), \mathcal{W} is the channel bandwidth (refer Table 2 for details), $L_{\text{implementation}}$ is the implementation loss (10 dB as assumed in Kim and Molisch⁹), and F_N is the noise figure (5 dB as also assumed and used in Kim and Molisch⁹).

In addition, Table 2 shows the parameter settings for transmit power, transmit antenna gain, receive antenna gain, and channel bandwidth in each carrier frequency.

Performance of fair connection

For performance comparison, a received signal strength indicator (RSSI)-based association algorithm is also simulated along with the proposed fair connection. With the RSSI-based association algorithm, each MU finds its AU which can provide the maximum RSS. In each unit time, one MU is added and the MU performs the connection procedures as follows: (1) RSSI-based algorithm and (2) the proposed fair algorithm. Eventually, 100 MUs will be deployed into the

Table 2. Parameters.

Parameters	Description	Setting
$P_i^{\text{Tx}}[t]$	Transmit power	19 dBm (maximum) and 10 dBm (minimum)
G_i^{Tx} and G_j^{Rx}	Transmit/receive gains	24.5 dBi in 28 GHz, 38 GHz, and 60 GHz ¹⁹
$\mathcal{W}_{i \rightarrow j}$	Bandwidth	1400 MHz in 28 GHz, 800 MHz in 38 GHz, ⁹ and 2160 MHz in 60 GHz ²⁰

Algorithm 1. Fair connection at MUs

```

while [(1) AU breaking down, or (2) new MU joining]
do
    • Find the set of nearby AUs ( $S_j$ ), that is,  $AU_i$  where
       $\forall i \in S_j$ 
    • Observe the following parameters from the nearby
      AUs, that is,
       $AU_i$  where  $\forall i \in S_j$  at time  $t$ 
       $\mathcal{W}_{i \rightarrow j}$ ,  $P_{i \rightarrow (j)}^{\text{Rx}}[t]$ ,  $B_i[t]$ , and  $N_i[t]$ 
    • Calculate  $K_i[t]$  with
      
$$\frac{\mathcal{W}_{i \rightarrow j} \log_2 \left( 1 + \frac{P_{i \rightarrow (j)}^{\text{Rx}}[t]}{N_0} \right)}{B_i[t] \cdot (N_i[t] + 1)}$$

      for all nearby AUs, that is,
       $AU_i$  where  $\forall i \in S_j$ 
    • Select the maximum  $K_i[t]$  and make a connection with
      the corresponding  $AU_i$ 
end

```

network. With this given setting, the simulation runs as follows. For each unit time (from $t = 1$ to $t = 100$), the proposed fair association algorithm and RSSI-based association algorithm are executed. Then, as observed, the average standard deviation of buffer backlogs at all AUs in both fair association and RSSI-based association algorithms is observed, and this operation is conducted for 50 times with random AU and MU deployments. After that, the standard deviation distribution can be obtained for the 50 iterations. Finally, sorted results of the distribution can be calculated. The results are in Figure 4.

In Figure 4, the x-axis and y-axis stand for the number of iterations and standard deviation values for each iteration, respectively. As shown in Figure 4, the proposed fair association has the lower standard deviation distribution compared to the RSSI-based association. This means that the proposed algorithm shows better performance with respect to fairness. Even when both algorithms have the worst fairness, the proposed fair association shows 11.57% better performance than the RSSI-based association based on the following calculation

$$\frac{4.3346 - 3.8332}{4.3346} \times 100 = 11.57\% \quad (25)$$

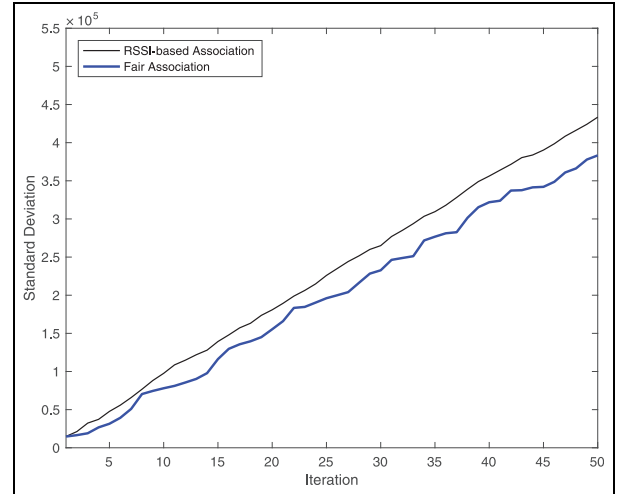
Algorithm 2. Dynamic buffering at AUs

```

while  $0 < t$  do
    • Given:  $d, V, \mathcal{W}, G_i^{\text{Tx}}, G_c^{\text{Rx}}, N_0, B_i[0] = 0$ 
    • Observe  $B_i[t]$ 
    • Calculate  $O(d)$  and  $PL(d)$ 
    • Calculate the amount of power allocation  $\mathcal{P}_i^{\text{Tx}}[t]$  with
      
$$\frac{\mathcal{W}V}{\ln 2} B_i[t] - N_0 \frac{10^{\frac{O(d) + PL(d)}{10}}}{10^{\frac{G_i^{\text{Tx}} + G_c^{\text{Rx}}}{10}}}$$

    • Adjust  $\mathcal{P}_i^{\text{Tx}}[t]$  with equation (23)
    •  $t \leftarrow t + 1$ 
end

```

**Figure 4.** Simulation results of fair association.

Performance of dynamic buffering

To verify the performance of the proposed dynamic buffering, simulations are performed with two different tradeoff coefficients, that is, $V = 10^{-3}$ and $V = 3 \times 10^{-3}$. In addition, the proposed dynamic buffering is compared to static power allocation where the transmit power is set to maximum (i.e. 19 dBm) or minimum (i.e. 10 dBm). Finally, four buffering algorithms are discussed in this section, including (1) dynamic buffering with $V = 10^{-3}$, (2) dynamic buffering with $V = 3 \times 10^{-3}$, (3) max-power buffering, which is achieved with static maximum power allocation, and

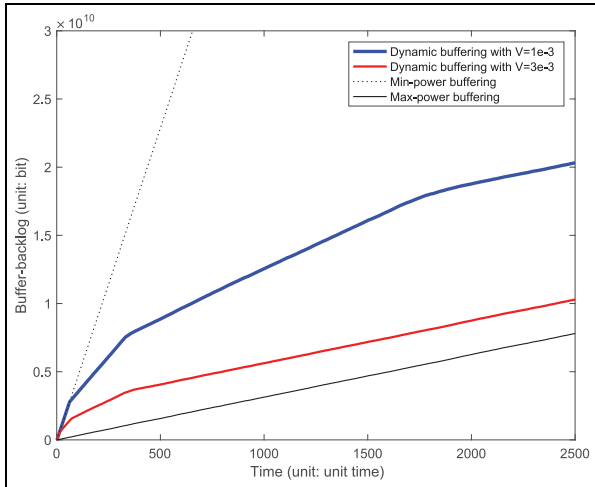


Figure 5. Simulation results of dynamic buffering.

(4) min-power buffering, which is achieved with static minimum power allocation, respectively.

With the given four algorithms, run-time simulations are conducted during 2500 unit times. While doing the simulations, the summation of buffer-backlog sizes of all deployed AUs is observed. As a result, Figure 5 presents the corresponding simulation results with these given buffering algorithms where x -axis and y -axis stand for the running time of simulations and the summation of buffer-backlog sizes of all AUs, respectively.

As presented in Figure 5, max-power buffering shows the most stable behavior because it always processes a lot of bits from the buffers of AUs. However, min-power buffering shows the most unstable behavior. Between the two behavior curves, two dynamic buffering algorithms are located. As formulated, dynamic buffering is much more conservative in terms of buffer occupancy when it has higher V values. As expected, Figure 5 shows that dynamic buffering with higher V (i.e. $3 \times 10^{-3} > 10^{-3}$) is more stable in terms of buffer-backlog sizes. More interestingly, it can be observed that dynamic buffering algorithms process less bits in early stages (i.e. the slopes of two curves are aggressive in early stages and this means that buffer occupancies increase aggressively). This is in part because the buffer occupancies are not high in terms of packet overflows in early stages. Therefore, the dynamic buffering algorithms are concerned with power saving by allocating minimum powers at that time slots. When the buffers start to be filled with bits, dynamic buffering algorithms dynamically control power allocation under the observation of buffer occupancy in order to avoid packet overflows. Therefore, the algorithms start to consider buffer sizes in the middle of the operation. Therefore, they start to process more bits.

Concluding remarks and future work

In this article, two reliable algorithms are proposed in cloud-assisted SNS platforms: a fair connection in each MU and a dynamic buffering in each AU. For *fair connection in each MU*, a novel re-association algorithm is proposed that works based on (1) the buffer-backlog sizes in each AU to avoid overflows, (2) the number of associated MUs in each AU, and (3) different bandwidths. For *dynamic buffering in each AU*, a stochastic algorithm is designed that works based on the buffer backlog in each AU over 60 GHz links while preserving buffer stability. The simulation results present the proposed two algorithms achieve desired performance. In terms of fair association, the proposed algorithm shows 11.57% performance improvements in the aspects of standard deviation of buffer backlogs in each AU. In terms of dynamic buffering, the proposed algorithm shows desired performance improvements compared to static buffering algorithms.

As a future work, we will explore the following directions:

- We will look into the response time of each mobile unit, incorporate it into our algorithms, and look into how much it can introduce of a communication overhead.
- We will conduct further simulation results in other settings, including large-scale simulation networks which would potentially result in more interest observations.

Declaration of conflicting interests

The author(s) declared no potential conflicts of interest with respect to the research, authorship, and/or publication of this article.

Funding

The author(s) disclosed receipt of the following financial support for the research, authorship, and/or publication of this article: This research was supported by Chung-Ang University Research Grant (2017) and partially supported by National Research Foundation of Korea (Grant No. 2016R1C1B1015406).

References

1. Mohaisen A, Kune DF, Vasserman EY, et al. Secure encounter-based mobile social networks: requirements, designs, and tradeoffs. *IEEE T Depend Secure* 2013; 10(6): 380–393.
2. Wu J and Wang Y. Hypercube-based multipath social feature routing in human contact networks. *IEEE T Comput* 2014; 63(2): 383–396.

3. Shen H, Liu J, Chen K, et al. SCPS: a social-aware distributed cyber-physical human-centric search engine. *IEEE T Comput* 2015; 64(2): 518–532.
4. Xiao M, Wu J and Huang L. Community-aware opportunistic routing in mobile social networks. *IEEE T Comput* 2014; 63(7): 1682–1695.
5. Zhang D, Zhang D, Xiong H, et al. NextCell: predicting location using social interplay from cell phone traces. *IEEE T Comput* 2015; 64(2): 452–463.
6. Hur S, Kim T, Love D, et al. Multilevel millimeter wave beamforming for wireless backhaul. In: *Proceedings of the IEEE global communications conference (GLOBECOM) workshops*, Houston, TX, USA, 5–9 December 2011, pp.253–257. New York: IEEE.
7. Rappaport T, Gutierrez F, Ben-Dor E, et al. Broadband millimeter-wave propagation measurements and models using adaptive-beam antennas for outdoor urban cellular communications. *IEEE T Antenn Propag* 2013; 61(4): 1850–1859.
8. Azar Y, Wong G, Wang K, et al. 28 GHz propagation measurements for outdoor cellular communications using steerable beam antennas in New York city. In: *Proceedings of the IEEE international conference on communications (ICC)*, Budapest, Hungary, 9–13 June 2013, pp.5143–5147. New York: IEEE.
9. Kim J and Molisch AF. Quality-aware millimeter-wave device-to-device multi-hop routing for 5G cellular networks. In: *Proceedings of the IEEE international conference on communications (ICC)*, Sydney, NSW, Australia, 10–14 June 2014, pp.5251–5256. New York: IEEE.
10. Lee W, Kim E, Kim J, et al. Movement-aware vertical handoff of WLAN and mobile WiMAX for seamless ubiquitous access. *IEEE T Consum Electr* 2007; 53(4): 1268–1275.
11. Zheng K, Meng H, Chatzimisios P, et al. An SMDP-based resource allocation in vehicular cloud computing systems. *IEEE T Ind Electron* 2015; 62(12): 7920–7928.
12. Yu R, Huang X, Kang J, et al. Cooperative resource management in cloud-enabled vehicular networks. *IEEE T Ind Electron* 2015; 62(12): 7938–7951.
13. Wu H, Lou L, Chen CC, et al. Cloud-based networked visual servo control. *IEEE T Ind Electron* 2013; 60(2): 554–566.
14. Kim J. *Elements of next-generation wireless video systems: millimeter-wave and device-to-device algorithms*. PhD Dissertation, University of Southern California, Los Angeles, CA, 2014.
15. Kim J. Energy-efficient dynamic packet downloading for medical IoT platforms. *IEEE T Ind Inform* 2015; 11(6): 1653–1659.
16. ITU. *Attenuation by atmospheric gases*. ITU-R P.676-10, September 2013, https://www.itu.int/dms_pubrec/itu-r/rec/p/R-REC-P.676-10-201309-S!!PDF-E.pdf
17. Hong S-N and Kim J. Joint coding and stochastic data transmission for uplink cloud radio access networks. *IEEE Commun Lett* 2014; 18(9): 1619–1622.
18. Kim J and Lee W. Stochastic decision making for adaptive crowdsourcing in medical big-data platforms. *IEEE T Syst Man Cy: S* 2015; 45(11): 1471–1476.
19. Rappaport TS, Sun S, Mayzus R, et al. Millimeter wave mobile communications for 5G cellular: it will work! *IEEE Access* 2013; 1: 335–349.
20. Kim J, Tian Y, Mangold S, et al. Quality-aware coding and relaying for 60 GHz real-time wireless video broadcasting. In: *Proceedings of the IEEE international conference on communications (ICC)*, Budapest, 9–13 June 2013, pp.5148–5152. New York: IEEE.